DECEMBER 2018

SAN FRANCISCO ESTUARY & WATERSHED SCIENCE

Sponsored by the Delta Science Program and the UC Davis John Muir Institute of the Environment

RESEARCH

Hourly Analyses of the Large Storms and Atmospheric Rivers that Provide Most of California's Precipitation in Only 10 to 100 Hours per Year

Maryam A. Lamjiri*[1], Michael D. Dettinger[1,2], F. Martin Ralph[1], Nina S. Oakley[1,3], and Jonathan J. Rutz[4]

Volume 16, Issue 4 | Article 1
https://doi.org/10.15447/sfews.2018v16iss4art1

* Corresponding author email: *masgaril@ucsd.edu*

1 Center for Western Weather and Water Extremes
Scripps Institution of Oceanography
University of California, San Diego
La Jolla, CA 92093 USA

2 U.S. Geological Survey
Carson City, NV 89701 USA

3 Desert Research Institute
University of Nevada, Reno
Reno, NV 89523 USA

4 Science and Technology Infusion Division
National Weather Service
Western Region Headquarters
Salt Lake City, UT 84102 USA

ABSTRACT

California is regularly affected by floods and droughts, primarily as a result of too many or too few atmospheric rivers (ARs). This study analyzes a 2-decade-long hourly precipitation data set from 176 California weather stations and a 3-hourly AR chronology to report variations in rainfall events across California and their association with ARs. On average, 10–40 and 60–120 hours of rainfall in southern and northern California, respectively, are responsible for more than half of annual rainfall accumulations. Approximately 10% to 30% of annual precipitation at locations across the state is from only one large storm. On average, northern California receives 25 to 45 rainfall events annually (40% to 50% of which are AR-related). These events typically last longer and have higher event-precipitation totals than those in southern California. Northern California also receives more AR landfalls with longer durations and stronger Integrated Vapor Transport (IVT). On average, ARs contribute 79%, 76%, and 68% of extreme-rainfall accumulations (i.e., top 5% events annually) in the north coast, northern Sierra, and Transverse Ranges of southern California, respectively.

The San Francisco Bay Area terrain gap in the California Coast Range allows more AR water vapor to reach inland over the Delta and Sacramento Valley, and thus influences precipitation in the Delta's catchment. This is particularly important for extreme precipitation in the northern Sierra Nevada, including river basins above Oroville Dam and Shasta Dam.

This study highlights differences between rainfall and AR characteristics in coastal versus inland northern California – differences that largely determine the regional geography of flood risks and water reliability. These analyses support water resource, flood, levee, wetland, and ecosystem management within the catchment of the San Francisco Estuary system by describing regional characteristics of ARs and their influence on rainfall on an hourly time-scale.

KEY WORDS

California precipitation, atmospheric rivers, hourly rainfall characteristics, extreme rainfall, flood, San Francisco Bay Area, Sierra Nevada

1 INTRODUCTION

California's precipitation is vital to its people, agriculture, and ecosystems—and dictates its frequent flooding and (when lacking) droughts. A large part of California's annual precipitation totals arrives in only a few large storms, which introduces large interannual rainfall variability (Dettinger et al. 2011). The large storms are most often associated with atmospheric rivers (ARs) that are long, narrow regions of intense horizontal water vapor transport, typically associated with extratropical cyclones (Zhu and Newell 1998; Ralph et al. 2004, 2006, 2018a; Neiman et al. 2008; Dettinger et al. 2011; Rutz et al. 2014; Waliser and Guan 2017; Glossary of Meteorology 2017).

Many previous studies have documented the effects of ARs on extreme precipitation and flooding around the world (Dettinger and Ingram 2013; Lavers et al. 2013; Lavers and Villarini 2015; Waliser and Guan 2017; Paltan et al. 2017). Particularly over the US West Coast, ARs contribute greatly to annual precipitation accumulation and streamflow generation (Neiman et al. 2008; Guan et al. 2010; Dettinger et al. 2011; Kim et al. 2013; Konrad and Dettinger 2017), and play a critical role in ending drought episodes (Dettinger 2013). ARs are also responsible for extreme precipitation and major floods as well as flash floods, landslides, and debris flows in this region (Ralph et al. 2006, 2013; Neiman et al. 2011; Dettinger and Ingram 2013; Lamjiri et al. 2017; Young et al. 2017; Oakley et al. 2017).

Lavers et al. (2016) have demonstrated that, at lead times of several days, water vapor transport—a defining characteristic of ARs—can be predicted more accurately than precipitation. This ability to better forecast ARs, together with the critical influence of ARs on California's water resources, has inspired many efforts to integrate AR forecasts into reservoir-management strategies (FIRO Steering Committee 2017). In utilizing AR forecasts, it is important to identify region-specific precipitation characteristics of—and responses to—variations in AR characteristics. Such characteristics may include AR orientations, durations, or intensities; and variations may yield extreme precipitation and floods in one region, while causing only moderate or weak precipitation over nearby areas (Ralph et al. 2003; Neiman et al. 2011; Hughes et al. 2014). An important example of this is the role of the gap in coastal terrain near the San Francisco Bay, which recent studies have found allows greater water vapor transport in ARs to penetrate inland into the Central Valley and enhance precipitation in the Sierras (Neiman et al. 2013; White et al. 2015). These studies are particularly important in California, where future increases in heavy precipitation and horizontal water vapor transport are projected in a warming climate (Dettinger 2011; Lavers et al. 2013; Warner et al. 2014; Dettinger 2016; Hagos et al. 2016; Polade et al. 2017; Espinoza et al. 2018).

Most studies have explored California's precipitation using 6-hourly, daily, 3-day, monthly, or longer time-scales of precipitation. As a result, some temporal characteristics of individual precipitation events such as duration have been only coarsely resolved. To extend understanding of such precipitation characteristics and their association with ARs, this study analyzes 2 decades of hourly precipitation observations from 176 California weather stations in the context of a 3-hourly AR chronology. In particular, this study addresses three questions:

1. Which regions in California receive the most extreme rainfall events, and how do rainfall characteristics differ regionally?
2. What is the contribution of ARs to rainfall and extreme rainfall events at hourly time-scales?
3. How does extreme rainfall in different regions depend on the intensity of arriving ARs?

Precipitation extremes are central to California's water resources, floods, and ecosystems, and the more precisely we understand their details, the better we will be able to anticipate and manage the state's resources and hazards.

2 DATA AND METHODOLOGY

2.1 Hourly Rainfall Observations

This study uses a data set of quality controlled hourly rainfall observations from the Remote Automated Weather Station (RAWS) network (Brown et al. 2011) produced by Oakley et al. (2018). The data set contains observations from 137 RAWS stations that have at least 80% complete October–May data between 1995–2016. While all measurements of precipitation in any month are analyzed here, the requirement that missing measurements be limited is based on October–May records because most of the annual precipitation in California falls during that season. RAWS began as a fire-weather network and its stations tend to be located in remote areas with high-altitude, complex terrains that typically are not well sampled by other networks, which instead focus more on population centers and transportation corridors (Myrick and Horel 2008). Thus, the RAWS network provides useful information in areas where much of California's precipitation falls.

In addition to the RAWS data set, hourly precipitation observations from California Irrigation Management Information System (CIMIS; *http://www.cimis.water.ca.gov/*) are included to provide coverage in the Central Valley and other agricultural areas. These observations are processed for quality and accuracy, and flagged accordingly, before being stored in the CIMIS database. After removing observations flagged as missing or inaccurate, 39 CIMIS stations are also included here. Thus, the 176 RAWS and CIMIS stations cover most regions in California; however, gaps exist in the southeastern deserts, and no coverage in the high elevations of the Sierra Nevada where the presence of snowfall is a complicating issue.

Precipitation gauges in the RAWS and CIMIS networks are unheated and thus are unreliable monitors of frozen precipitation. All of the 176 stations are located below the mean freezing level (1,700 m) in the Sierra Nevada, to reduce measurement problems associated with snowfall and subsequent melt. Furthermore, precipitation measurements coincident with air temperatures below 0°C (as an estimate of frozen precipitation) are excluded from the analysis. Therefore, the focus of the current study is precipitation in the form of rainfall rather than snow.

2.2 Chronology of California's AR Landfalls

In recent years, research groups using differing detection algorithms and data sets have developed a number of different AR chronologies (Ralph et al. 2018b; Shields et al. 2018). The AR landfall chronology this study uses is based on the methodology of (Rutz et al. 2014) as applied to the NASA Modern-Era Retrospective analysis for Research and Applications (MERRA-2) data set with 3-hourly temporal resolution and 0.5° latitude by 0.625° longitude spatial resolution (retrieved from *http://www.inscc.utah.edu/~rutz/ar_catalogs/merra_0.5/*). This chronology offers a high temporal and spatial resolution that is important for the current study to capture AR variability in relation to hourly precipitation.

The methodology of (Rutz et al. 2014) catalogs ARs as features in vertically integrated vapor transport (IVT) fields that have IVT rates $\geq 250\,\mathrm{kg\,m^{-1}s^{-1}}$ and are at least 2,000 km long. This catalog was compared with a number of other leading AR catalogs and key re-analyses, and was found to represent other analogous AR detection tools (Ralph et al. 2018).

In the current study, an "AR event" is defined as the continuous presence of AR conditions above a grid point. Based on this definition, ARs may exist for only one 3-hourly time-step and still be considered an event. This allowance for shorter-duration AR events is applied for two reasons: (1) rainfall events are defined based on hourly observations and are not required to meet a minimum duration requirement (see Section 2.3, "Delineation of Rainfall and Extreme Rainfall Events"). Therefore, for consistency, inclusion of very short AR events is preferred, and (2) requiring that AR events be arbitrarily long would significantly reduce their perceived frequencies, more so in inland than coastal regions, and would result in under-attribution of rainfall events to AR influences.

2.3 Delineation of Rainfall and Extreme Rainfall Events

Using hourly rainfall observations for the period of 1995–2016, and following the methodology of

https://doi.org/10.15447/sfews.2018v16iss4art1

Lamjiri et al. (2017), a "rainfall event" is defined here as a period of continuous rainfall with at least 5 mm of rain accumulation over the total event period. As delineated here, a rainfall event is separated from others by at least 6 hours with no precipitation. For each rainfall event, event-total rainfall (mm) is defined as accumulated rainfall from the beginning to the end of the event; event-duration is the total number of hours with non-zero rainfall (h); event-average intensity is event-total rainfall divided by event-duration (mm h^{-1}); and event-maximum intensity is the largest hourly rate of rainfall during the event (mm h^{-1}). In this study, rainfall events with the 5% largest event-total rainfall annually are considered extreme. This 5% threshold is an arbitrary indication of large storms. However, we acknowledge that not all 95th percentile rainfall events yield severe hydrological effects or activate geomorphologic processes.

2.4 Delineation of AR-Related Rainfall

In this study, at each station, a rainfall event is considered to be "AR-related" if AR conditions are present over the MERRA grid cell nearest to the station during at least 50% of the duration of the rainfall event. Based on this definition, an AR-related rainfall event may overlap with one or more distinct AR events. Requiring the presence of AR conditions overhead, rather than considering landfall conditions at the nearest coastal grid point, is relatively restrictive. This criterion overlooks the fact that some ARs do not remain as coherent and continuous features once they penetrate inland, although still being related to the same atmospheric phenomenon and providing the same moisture (Albano et al. 2017). However, attending to AR conditions overhead avoids overestimation of AR effects on in-land extreme precipitation, because most ARs tend to decay by orographic rain-out over coastal regions, and result in less frequent and weaker AR conditions further inland. Moreover, coastal topography can directly affect inland penetration patterns of ARs, and, therefore, some inland areas might be more influenced by ARs than others, based on the location of gaps in the coastal topography.

Meeting the requirement of the presence of AR conditions during at least 50% of the duration of rainfall events is harder in northern than southern California, because rainfall events last longer in northern California (see "3.1 Characteristics of Rainfall and Extreme Rainfall Events, 1995–2016" and Figure 1C). Consequently, even though some long rainfall events include precipitation more accurately attributed to ARs, if they do not meet this criterion, they are misclassified as non-AR rainfall.

3 RESULTS

3.1 Characteristics of Rainfall and Extreme Rainfall Events, 1995–2016

There are important distinctions between characteristics of northern and southern California rainfall events (north and south of 37.5°N, respectively, following the methodology of Kim et al. [2013]). These distinctions result in different associated hydrologic effects, and require adjusted water- and flood-management strategies. In general, northern California receives more than twice as many rainfall events per year (25 to 45) as southern California (2 to 15; Figure 1A). Rainfall events in northern California generate a median of 10–22 mm rainfall per event, where higher values of event-totals are associated with events along the north coast and some stations in the northern Sierra and northern Central Valley. Rain-shadowed regions of north-easternmost California generally experience smaller rainfall events, with a median of 8–10 mm rainfall generated per event. Southern California rainfall events have lower median event-totals (10–14 mm per event) than those in northern California (10–22 mm per event), with the exception of some parts of the Transverse Ranges, which receive a median of 20 mm rain per event (Figure 1B).

Rainfall events in northern California are significantly more persistent (at 95% confidence level, based on the Mann–Whitney U test [Mann and Whitney 1947]) than those in southern California, with median event durations in the range of 10–14 and < 5–11 hours, respectively. Rainfall events are particularly more persistent along the north coast (with median event-duration of 13 to 14 hours; Figure 1C), where frequent AR landfall occurs every year during the cool season. These ARs usually yield relatively long and moderately intense rainfall events in this region.

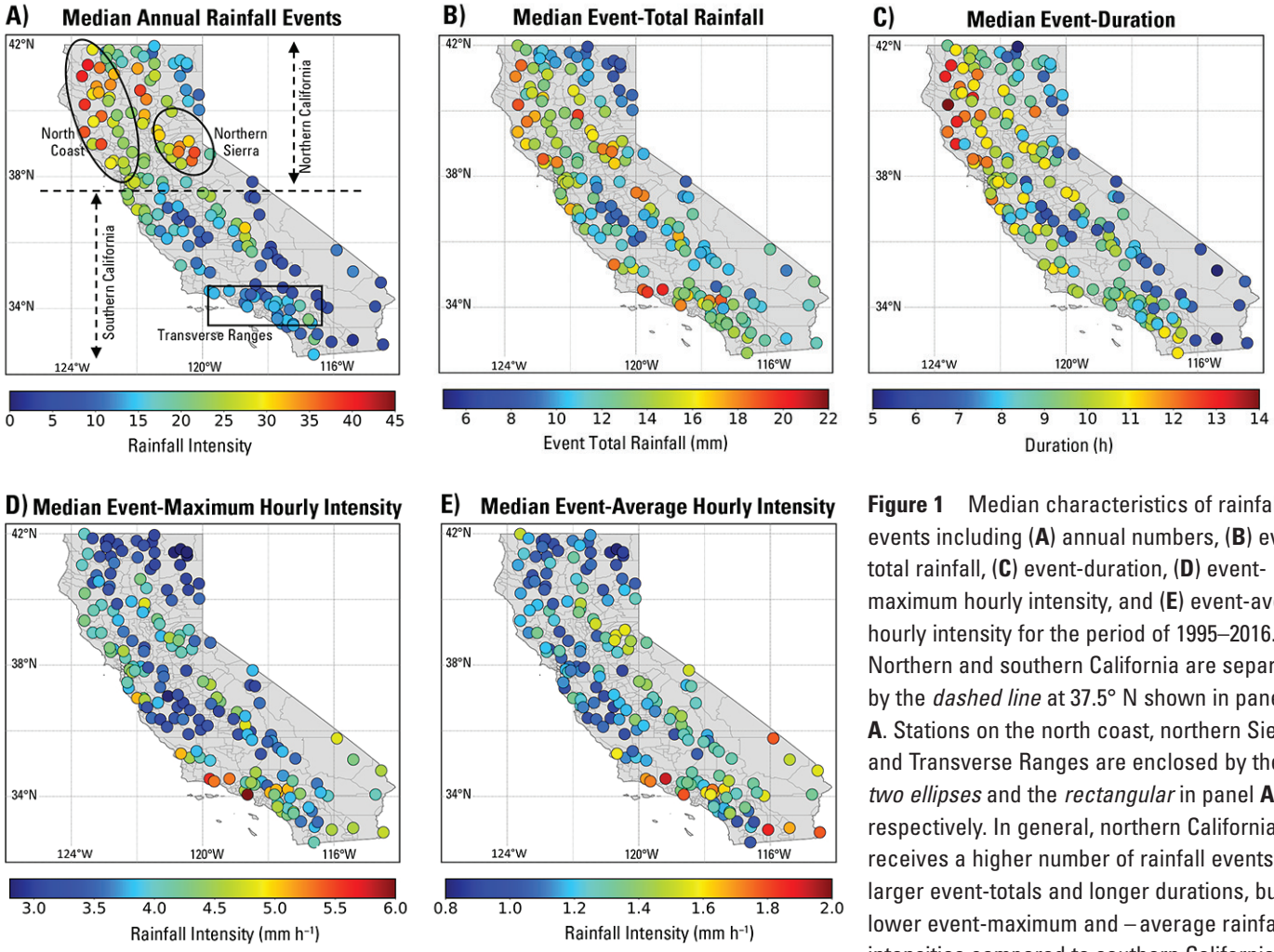

Figure 1 Median characteristics of rainfall events including (**A**) annual numbers, (**B**) event-total rainfall, (**C**) event-duration, (**D**) event-maximum hourly intensity, and (**E**) event-average hourly intensity for the period of 1995–2016. Northern and southern California are separated by the *dashed line* at 37.5° N shown in panel **A**. Stations on the north coast, northern Sierra, and Transverse Ranges are enclosed by the *two ellipses* and the *rectangular* in panel **A**, respectively. In general, northern California receives a higher number of rainfall events with larger event-totals and longer durations, but lower event-maximum and –average rainfall intensities compared to southern California.

Median values of event-maximum, and event-average rainfall intensities are significantly (at 95% confidence level, based on the Mann-Whitney U test) greater in southern (3.5–6 mm h^{-1} and 1.0–2.0 mm h^{-1}, respectively) than northern California (3–4.5 and 0.8–1.6 mm h^{-1}, respectively; Figures 1D and 1E). High-intensity rainfall events in southern California are mostly related to short-duration, high-intensity thunderstorms in the summer and autumn seasons. Because of a lower number of rainfall events per year in southern California, and the shorter duration associated with these events, annual total rainfall is much lower in this region than in northern California. Southern California, and the Transverse Ranges in particular, regularly suffer flash floods, shallow landslides, and debris flow associated with short but intense rainfall events, while northern California experiences fewer instances of flash floods, but often faces regular river flooding associated with AR-driven rainfall (Oakley et al. 2017; Young et al. 2017).

Using daily data, Dettinger et al. (2011) determined that 50% of California's annual precipitation accumulation falls over the course of only 5 to 15 days (Figure 2A and 2B; from Figure 2C of Dettinger et al. [2011]). Using hourly observations, we extend these results for total rainfall, instead of total precipitation (i.e., not including snowfall), to show in Figure 2C that 50% of annual rainfall accumulation comes from only 10 to 40 and 60 to 120 non-zero rainfall hours in southern and northern California, respectively. In fact, the rainfall event with the largest event-total rainfall each year contributes a median of 15% of annual rainfall accumulation in northern California and more than 30% in

https://doi.org/10.15447/sfews.2018v16iss4art1

in northern California and more than 30% in southern California (Figure 2D). Converting the daily precipitation values by Dettinger et al. (2011) to hourlies by simply multiplying them by 24 hours per day (Figure 2A and 2B) overestimates the number of hours that contribute half of the total precipitation. This is mainly because a median rainfall event in California lasts less than 18 hours (Figure 1C). Consequently, the largest differences between Figures 2A and 2C are located over the (northeastern-most) parts of California with the shortest average rainfall events, lasting only 8 to 12 hours.

Lamjiri et al. (2017) used coarsely gridded (2° latitude by 2.5° longitude) hourly precipitation observations to show that along the U.S. West Coast, and especially in California, event-total rainfall is more strongly correlated with event-duration than with event-maximum or event-average intensity. Figure 3 is a generalized confirmation of that result using station-based observations. Kendall's Tau Correlation coefficients (*r*) are used here to allow for hourly precipitation data that is not necessarily normally distributed. The non-parametric correlations between event-total rainfall and duration range mostly from 0.5 to 0.7 across California (Figure 3A) with the exception of some rain-shadowed regions of the Central Valley and southeastern California, where correlation coefficients decline to about 0.3 to 0.5. Correlation coefficients between event-totals and event-maximum precipitation intensities decay from coastal (~0.5–0.65) to inland regions (~0.4–0.5). As Lamjiri et al. (2017) found, correlation coefficients

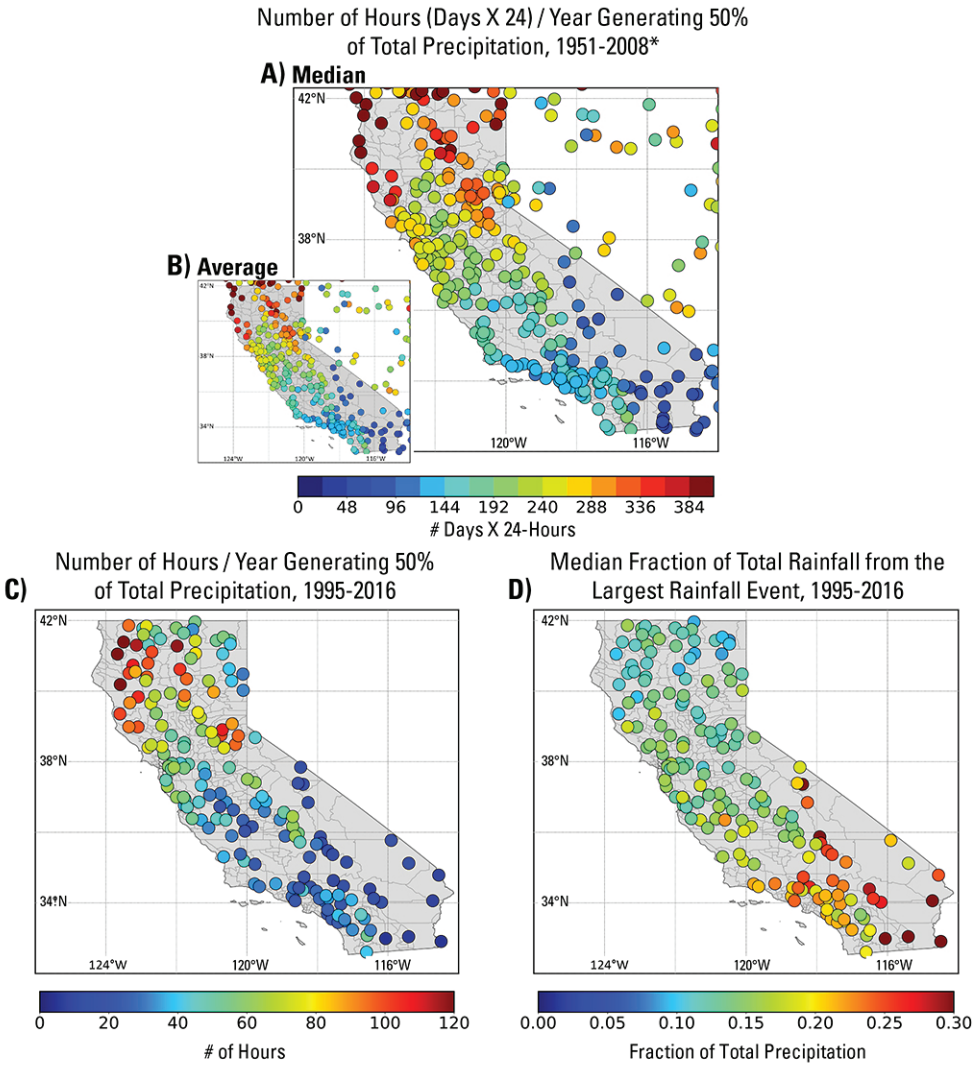

Figure 2 (**A**) Median and (**B**) average number of hours (days x 24) per year generating 50% of total precipitation, 1951–2008 (see Figure 2C in Dettinger et al. 2011), (**C**) median number of hours generating 50% of annual total rainfall, 1995–2016, and (**D**) median fraction of annual total rainfall from the largest rainfall event, 1995–2016. A large portion of annual rainfall totals in California falls during only a few hours, highlighting that California's large interannual variability of annual rainfall totals strongly depends on a few big storms.

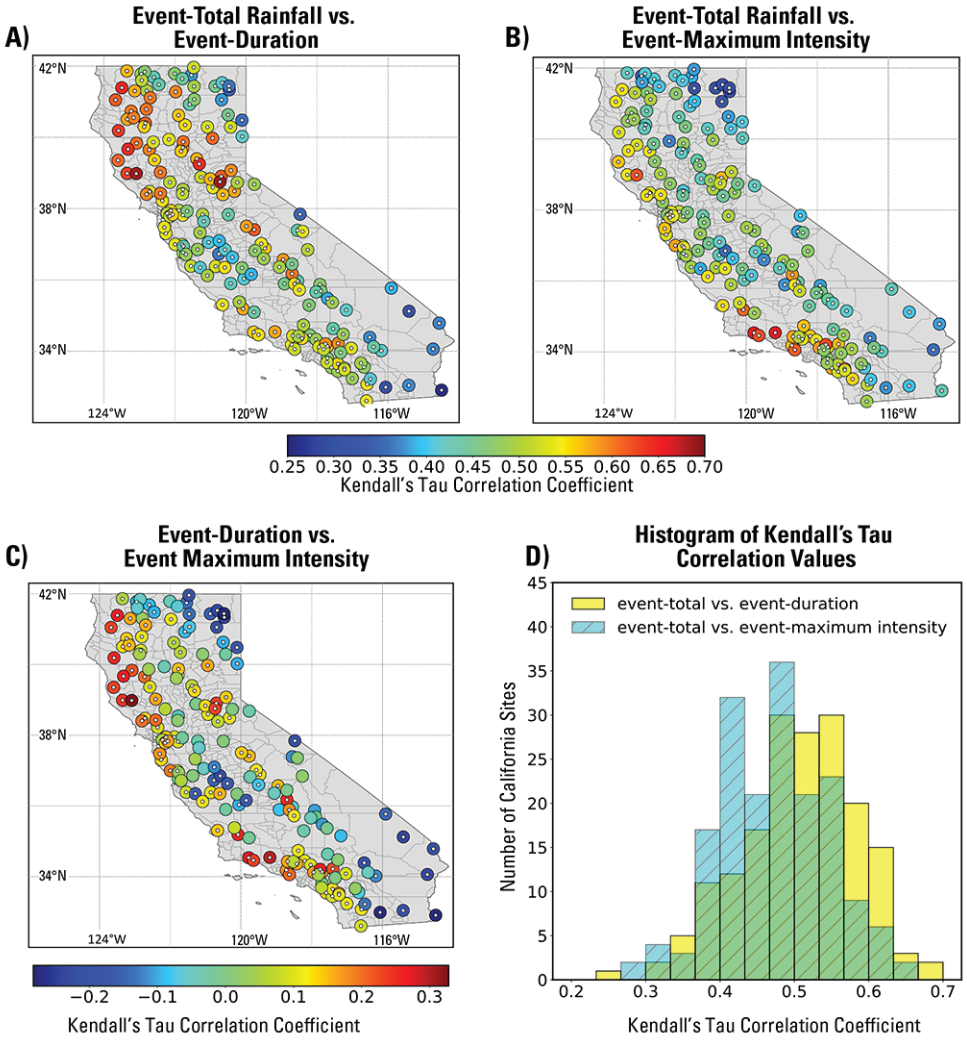

Figure 3 Kendall's Tau correlation coefficient between (**A**) event-total rainfall and event-duration, (**B**) event-total rainfall and event-maximum rainfall intensity, and (**C**) event-duration and event-maximum rainfall intensity. The histogram of correlation values in panels **A** and **B** are shown in panel **D**. Symbols with white dots in panels **A**, **B**, and **C** represent significant correlations at 95% confidence level. Event-totals are more strongly dominated by event-durations than by event-maximum intensities across California, except for some stations in the Transverse Ranges and southeastern California.

between event-total rainfall and event-duration are significantly (based on Kolmogorov–Smirnov tests) greater than those between event-total rainfall and event-maximum intensities (Figure 3D), especially in northern California. However, these findings are more subdued in the current study, where non-parametric statistics are used.

Relatively strong correlations between event-totals and event-maximum precipitation intensities, shown in Figure 3B, indicate that in addition to event-durations, event-maximum rainfall intensities play an important role in modulating event-total rainfall in coastal regions. Moreover, moderate yet significant (at 95% confidence level) correlations between event-durations and event-maximum intensities exist in the north coast, at some stations in the Sierra Nevada, and in the Transverse Ranges (Figure 3C). Therefore, longer rainfall events in these regions can also experience larger hourly intensities, and thus may lead to even greater event-total rainfall.

Median characteristics of extreme rainfall events compared to those from all rainfall events are shown in Figure 4. Based on the definition of extremes used in "2.3 Delineation of Rainfall and Extreme Rainfall Events," extreme rainfall events produce from 3 to more than 5 times larger event-total rainfall. Extreme rainfall events also last 1.5 to 4.5 times longer and have event-maximum intensities 1 to 2.5 times greater compared to median characteristics of all rainfall events. The ratio of the median of event-total rainfall from extreme events to the median value from all rainfall events in general

https://doi.org/10.15447/sfews.2018v16iss4art1

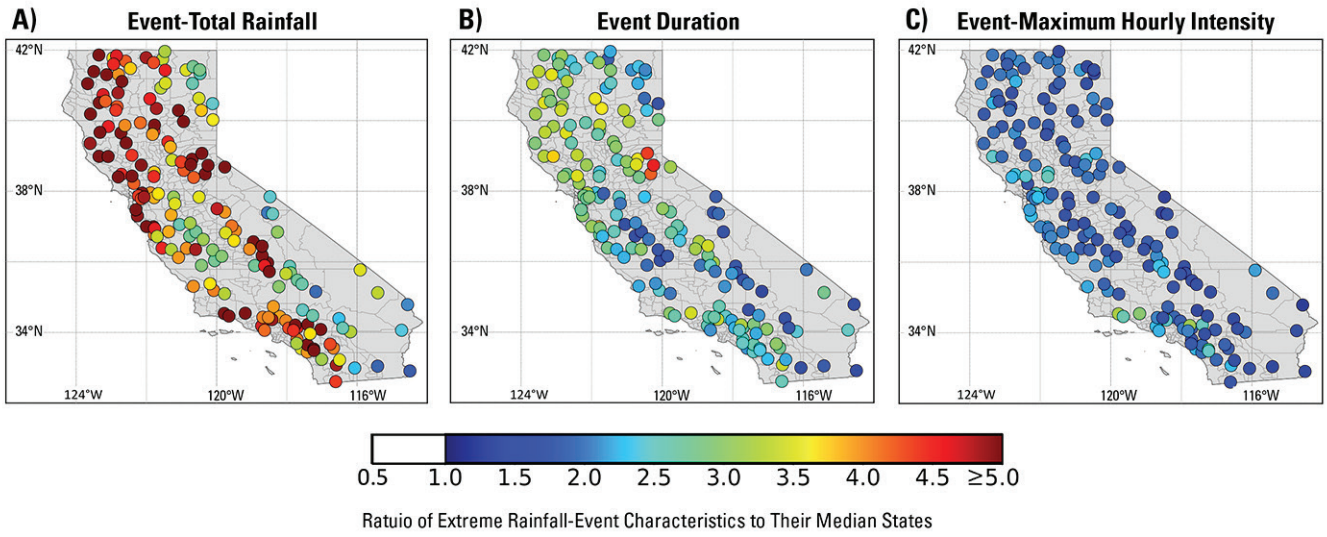

Figure 4 The ratio of median characteristics of extreme rainfall events relative to median values from all rainfall events for (**A**) event-total rainfall, (**B**) event-duration, and (**C**) event-maximum intensity. Extreme rainfall events are longer and more intense than median events across California, with larger differences associated with event-duration than with event-maximum intensity.

must, by the definition of extreme events, be greater than 1. Median event-durations and event-maximum intensities, however, are not necessarily constrained to be larger in extreme events. Nonetheless, the lack of white symbols in Figures 4B and 4C indicates that extreme rainfall events are almost always longer and more intense than rainfall events in general. Event durations are particularly long for extreme events across almost all of California.

3.2 Characteristics of AR Landfalls from 1995–2016

Figure 5 presents median characteristics of AR landfalls for the period of 1995–2016. The median number of AR events per year declines from 55 along the northern California coast to 10 in southern California (Figure 5A). In general, AR events persist overhead for a median of 12 hours along the north coast compared to about 9 hours in the southern Sierra Nevada and southern California (Figure 5B). Median AR event-maximum IVT values are greater than $400\,kg\,m^{-1}s^{-1}$ along the north coast and decline toward the southern Sierra Nevada and southern California, where average values are about 280 and $340\,kg\,m^{-1}s^{-1}$, respectively (Figure 5C). AR event-average IVT shows the same patterns as event-maximum IVTs but with lower magnitudes (Figure 5D). These AR characteristics (i.e., AR median event-duration and event-maximum and event-average IVT intensities) are significantly different (at 95% confidence level, based on the Mann–Whitney U test) in northern and southern California, where distinct rainfall characteristics are also observed, as discussed in "3.1 Characteristics of Rainfall and Extreme Rainfall Events, 1995–2016."

3.2.1 *Impacts of the San Francisco Bay Area Gap on Inland AR Characteristics*

One interesting feature—highlighted by the black oval in Figures 5A, 5C, and 5D—is the enhanced penetration of AR vapor through the gap in the coastal terrain near 38°N, referred to as the San Francisco Bay Area (SFBA) gap. Neiman et al. (2013) first linked the inland penetration of ARs through this gap to the precipitation distribution across the interior of northern California. They showed that as the low-level moisture from ARs penetrates through this gap, it contributes to the moistening and deepening of the Sierra Barrier Jet, which transports the moisture northward up to the Central Valley and yields precipitation in this region. White et al. (2015) documented that as a result of penetration of ARs through this gap, northern Sierra sites received precipitation compositions similar to those over coastal regions of northern California during AR

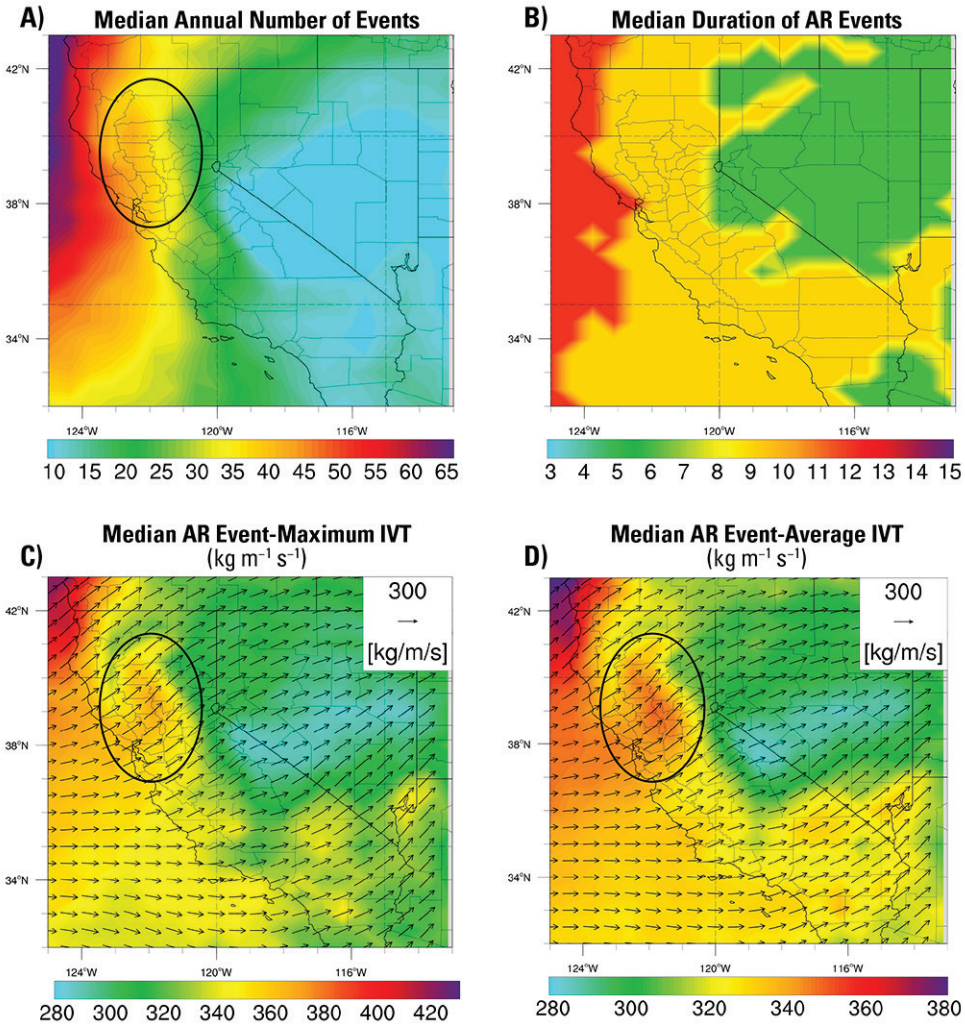

Figure 5 (**A**) Median annual number, (**B**) durations, (**C**) event-maximum IVT, and (**D**) event-average IVT of AR events, 1995–2016. The shading in panels **C** and **D** represent the median magnitude of AR event-maximum and average IVT fields (regardless of their directions), whereas the vectors represent the median direction of maximum and average IVT fields, with the length of vectors corresponding to the median magnitude of directional maximum and average IVT fields. The black ovals in panels **A**, **C**, and **D** indicate the penetration of ARs through the SFBA gap.

landfalls. In Figures 5A, C, and D, using a high-spatial-resolution AR chronology, we extend these results and highlight the enhancement of inland AR vapor transport through the SFBA gap based on the composite characteristics of AR events. Because ARs penetrate through this gap, a region of more frequent AR landfalls with higher maximum and average IVT intensities originates from the gap and reaches inland and northward up to the northern Central Valley. Seasonal analysis of AR characteristics over California (not shown here) confirms the presence of this region of intense AR conditions during all seasons, but with greater duration and IVT intensities during December–January–February (DJF).

3.3 Contribution of ARs to California's Rainfall

About 10% to 30% of rainfall events in southern Sierra and southern California, to 40% to 55% of those in the northern Sierra and central and northern coastal regions, are associated with ARs (Figure 6A). These AR-related rainfall events contribute from 20% to 40% of annual rainfall accumulations in the southern Sierra and southern California, to up to 70% of those along the north coast (Figure 6B). Comparing values presented in Figure 6A and 6B highlights that AR-related rainfall events generally yield more event-total rainfall than non-AR rainfall events. We found in this study that the contribution of AR-related rainfall events to annual rainfall accumulations broadly agrees with that found by Rutz et al. (2014), but are slightly higher than those reported by Dettinger et al. (2011). These differences are likely produced by different AR chronologies used in these analyses, and different methodologies adopted to define rainfall events and attribute rainfall to ARs.

https://doi.org/10.15447/sfews.2018v16iss4art1

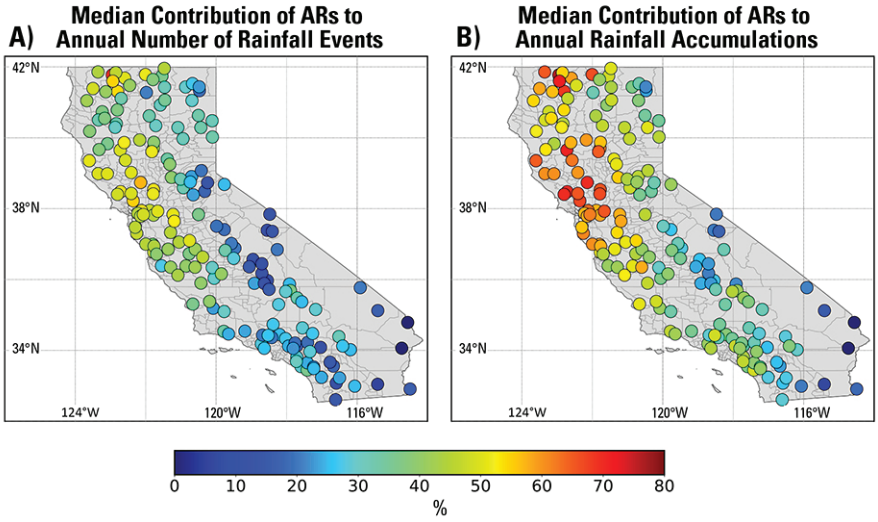

Figure 6 Median contribution of ARs to (**A**) the total number of rainfall events and (**B**) annual rainfall accumulations from all rainfall events at each station. Note that all rainfall events are required to generate at least 5 mm of rainfall per event. Rainfall events associated with ARs range from 10% in southern California to 55% in northern California, which contribute to 40% to more than 70% of annual rainfall totals in southern and northern California, respectively.

Nonetheless, the north–south gradient of AR contributions to annual precipitation accumulations is consistent with previous studies, with more contributions to northern than southern California precipitation accumulations. These results also highlight the decline in AR-related rainfall over the inland areas as a result of AR decay, in line with the findings of Rutz et al. (2014). The broad agreement between the findings of this study based on hourly rainfall observations and previous studies based on daily precipitation observations increases confidence in the use of both hourly and daily precipitation data sets.

Figure 7 compares median precipitation totals, durations, and maximum intensities of AR-related rainfall events with those from non-AR events. AR-related rainfall events are generally longer than non-AR events, especially in southern California. Maximum rainfall intensities associated with AR-related rainfall events are slightly higher than those of non-AR rainfall events, except for rain-shadowed regions of northeastern and southeastern California and the Central Valley. In general, AR-related rainfall events generate from 1.2 to more than 2.5 times more event-total rainfall than non-AR

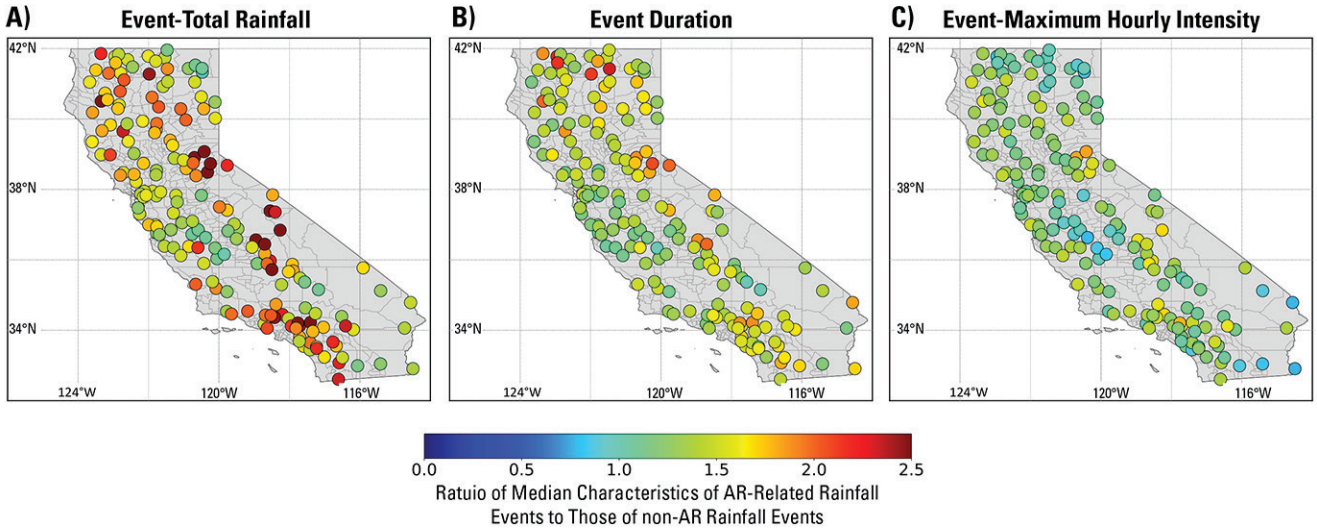

Figure 7 The ratio of median (**A**) event-total rainfall, (**B**) event-duration, and (**C**) event-maximum intensity of AR-related rainfall events to those of non-AR rainfall events. AR-related rainfall events are generally longer, with higher event-maximum intensities, and generate 1.2 to more than 2.5 times larger event-total rainfall than non-AR rainfall events.

events with greater ratios (more rainfall generated per AR event) in the Transverse Ranges and the Sierra Nevada.

3.4 Contribution of ARs to California's Extreme Rainfall

The previous sections addressed rainfall events, both large and small. Here, we turn to the largest 5% of rainfall events. Stations located in the north coast, northern Sierra, and the Transverse Ranges (shown in Figure 1A) experience the largest extreme rainfall-event totals in California. Overall, 77%, 71%, and 58% of extreme rainfall events over these regions are associated with ARs, respectively, which contribute 79%, 76%, and 68% of rainfall accumulations from all extreme rainfall events (Figure 8B).

The hourly data used here allows us to more precisely explore, in Figure 8C and Table 1, how AR-related extreme rainfall events over all three regions generate larger event-total rainfall than non-AR extreme events. Over the north coast and northern Sierra, AR-related extreme rainfall events are shorter, on average, than non-AR extreme events (Figure 8D). However, AR-related extreme rainfall events over these regions have larger maximum rainfall intensities and result in higher amounts of event-totals compared to non-AR extreme rainfall events.

Extreme rainfall events in the north coast and northern Sierra are generally longer than those in the Transverse Ranges, but have lower maximum (and average; not shown) rainfall intensities. In particular, the median duration of non-AR extreme rainfall events in the north coast and northern Sierra Nevada are 18 hours (86%) and 12 hours (57%) longer than those in the Transverse Ranges, while their maximum intensities are $1\,mm\,h^{-1}$ (13%) and $1.3\,mm\,h^{-1}$ (16%) lower, respectively. The considerably longer duration of non-AR extreme rainfall events in the north coast and northern Sierra Nevada results in higher median extreme precipitation totals in these regions compared to those in the Transverse Ranges (by 56% and 41%, respectively) even though they do not have rainfall intensities as high (Figure 8, Table 1). Unlike non-AR extreme rainfall events, the median duration of AR-related extreme events in the north coast and northern Sierra Nevada are only 35% and 23% longer than those in the Transverse Ranges. Maximum rainfall intensities of AR-related extreme events are larger in the Transverse Ranges than in the north coast and northern Sierra, which, combined with their relatively long durations, result in the largest AR-related extreme rainfall events in this region. Though the Transverse Ranges receive the largest extreme rainfall events, in general, such events are about three times less frequent in this region than in the north coast and northern Sierra Nevada.

Figure 9 shows averages of daily IVT and integrated water vapor (IWV, the total amount of water vapor in the atmosphere above a point on the surface) for days of AR-related extreme rainfall events. The IVT composite averages for extreme rainfall events over the northern Sierra, on average, are supported by a longer plume of more intense IVT than those associated with extreme rainfall events over the north coast and Transverse Ranges (Figures 9A–C). The IVT and IWV composites for the northern Sierra extreme events feature ARs that penetrate inland through the SFBA gap, and highlights the importance of this gap on extreme precipitation in the northern Sierra and northern Central Valley. IVT composites associated with extreme rainfall in the Transverse Ranges display weaker IVT intensities than those in the northern Sierra and north coast, partly because average IVT values are larger over northern than southern California, in general.

Daily-averaged 500-hPa geopotential height fields are also calculated and displayed as black contour lines in Figure 9 to illustrate the large-scale atmospheric-circulation patterns associated with AR-related extreme rainfall. The 500-hPa geopotential height composites feature a trough (where height contours bow southward) over the North Pacific, and a ridge (where height contours bow northward) over the western U.S. (Figures 9A and 9B). Winds about 5 km above sea level roughly follow these contours (on average during the AR-related rainfall extremes) so that this pattern indicates flows over the central California coast proceeding from southwest to northeast, perpendicular to the coastal mountain ranges in northern California. This pattern favors orographic precipitation enhancement in these regions. The 500-hPa geopotential height composite associated with extreme rainfall over the Transverse Ranges shows a deeper trough over the North Pacific (Figure 9C). This pattern favors southerly flow into

https://doi.org/10.15447/sfews.2018v16iss4art1

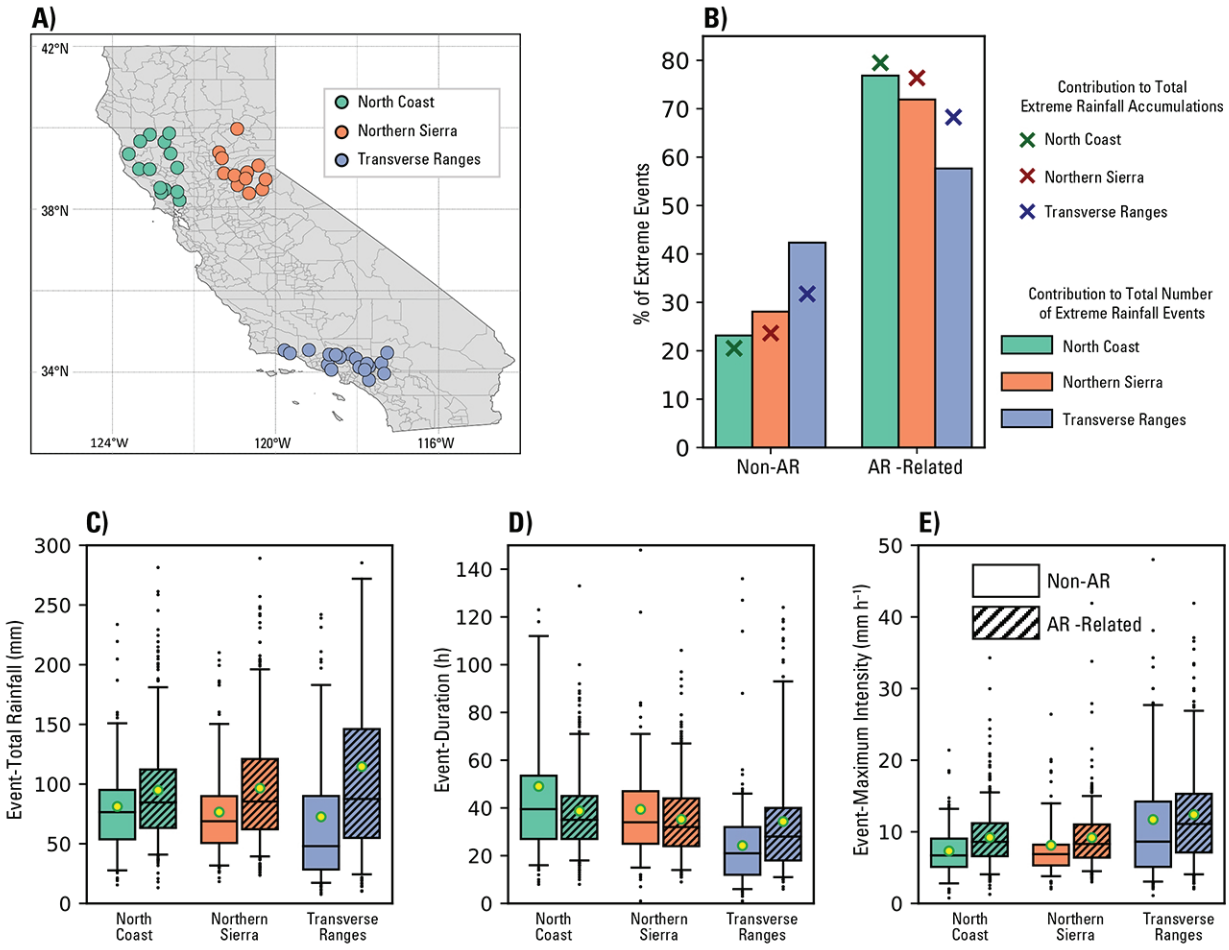

Figure 8 (**A**) Spatial map of stations on the north coast, northern Sierra, and Transverse Ranges, (**B**) percentages of extreme rainfall accumulations (bars) and number of extreme rainfall events (markers) associated with non-AR and AR-related extreme rainfall events, and box and whisker diagrams of (**C**) event-totals, (**D**) durations, and (**E**) maximum intensities of extreme rainfall. The solid-ground boxes in panels **C**, **D**, and **E** represent non-AR extreme rainfall events, whereas the hatched boxes represent those associated with ARs. The lower whisker, lower edge of the box, upper edge of the box, and the upper whisker represent 5th, 25th, 75th, and 95th percentiles, respectively. The median and mean of distributions are shown by horizontal black lines and yellow dots, respectively. Extreme rainfall events show distinct characteristics in different regions of California, with the Transverse Ranges AR-related extreme events generating the largest event-total rainfall and largest event-maximum intensities, compared to those on the north coast and northern Sierra.

Table 1 Median characteristics of AR and non-AR extreme events on the north coast, northern Sierra, and Transverse Ranges

	Median extreme event–total rainfall (mm)			Median extreme event–duration (h)			Median extreme event–maximum intensity (mm h^{-1})		
	AR	Non-AR	% Difference*	AR	Non-AR	% Difference*	AR	Non-AR	% Difference*
North Coast	82.2	76.0	7.5	35.0	39.0	–11.4	8.5	6.9	18.8
Northern Sierra	85.6	68.9	19.5	32.0	33.0	–3.1	8.3	6.6	20.4
Transverse Ranges	88.9	48.8	45.1	26.0	21.0	19.2	11.2	7.9	29.5

* % Difference= [(AR-related extreme rainfall characteristic) –(non-AR extreme rainfall characteristic)]/(AR-related extreme rainfall characteristic) ? 100.

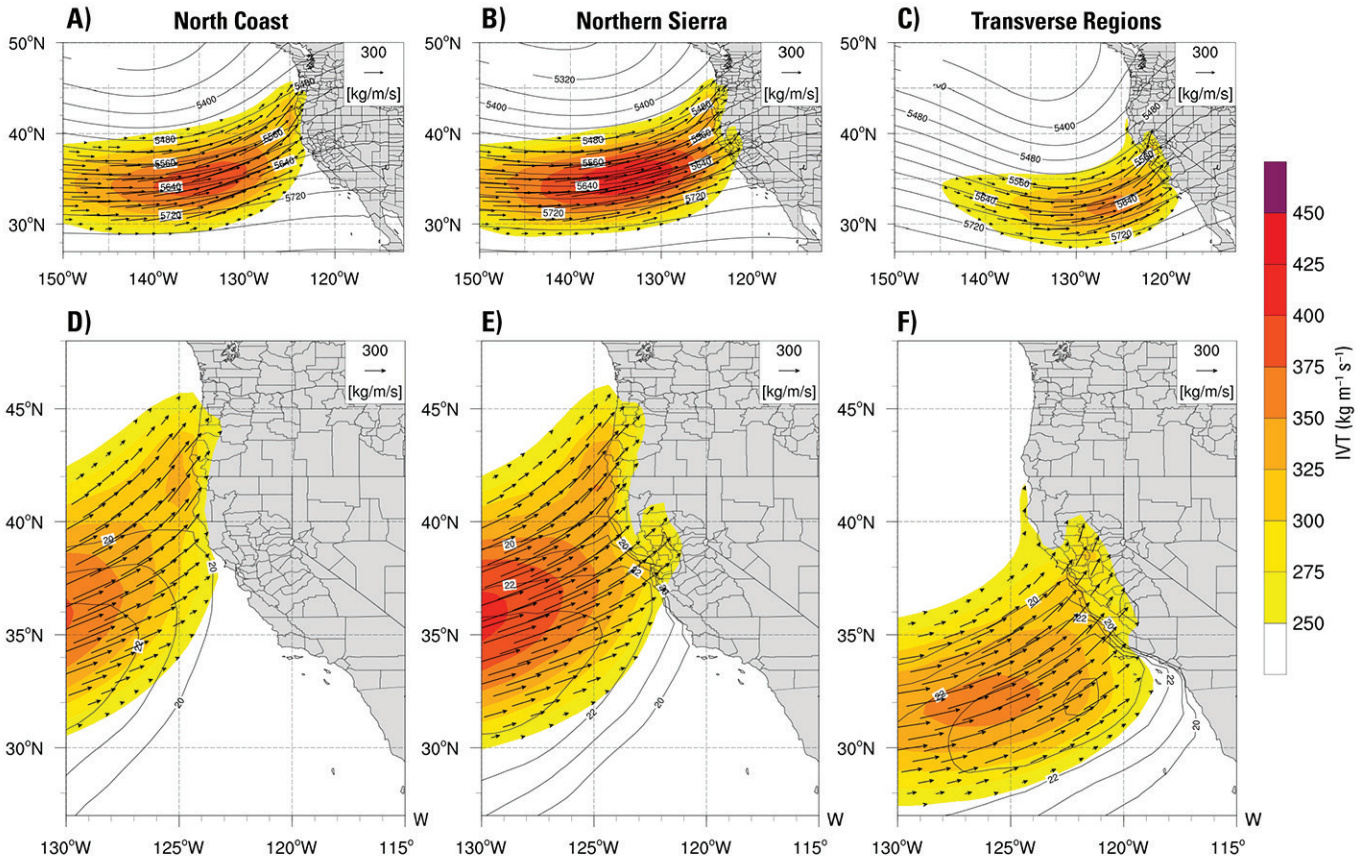

Figure 9 Composites of daily-averaged IVT (shadings) and 500-hPa geopotential height (contours) from the MERRA-2 reanalysis data set for days of AR-related extreme rainfall events over the (**A**) north coast (149 days), (**B**) northern Sierra (129 days), and (**C**) Transverse Ranges (73 days). Panels **D**, **E**, and **F** are similar to panels **A**, **B**, and **C**, but with contours representing MERRA-2 IWV composites instead of 500-hPa geopotential height.

the east–west oriented mountains of the Transverse Ranges, favorable for orographic precipitation in this region.

The largest differences between IVT composites of the northern Sierra and north coast exist at the SFBA gap (Figure 10). This highlights that—among ARs making landfall along the northern California coast—the difference between ARs producing extreme precipitation over the northern Sierra Nevada (and affecting the Delta) and those producing extreme precipitation over coastal regions of northern California, the greater penetration of IVT is through the SFBA gap. The SFBA gap and inland AR penetrations associated with it are important for the geography of flood risks and water reliability along the Sierra Nevada front and Central Valley. Weather forecasters have long recognized this, and it is an example of why not all ARs equally affect this part of California.

4 CONCLUSIONS

We analyzed roughly 2 decades (1995–2016) of hourly rainfall observations at 176 stations across California, as well as a 3-hourly AR landfall chronology, to describe how large storms—and especially ARs—affect California's rainfall regime. Our study complements the existing literature on California's precipitation and ARs by focusing on hourly characteristics of rainfall events and extremes, and on their links to ARs, a subject that has previously been addressed in less temporally resolved data sets and at regional scales. Using hourly observations, we find that annual rainfall in California is even more volatile than has been

https://doi.org/10.15447/sfews.2018v16iss4art1

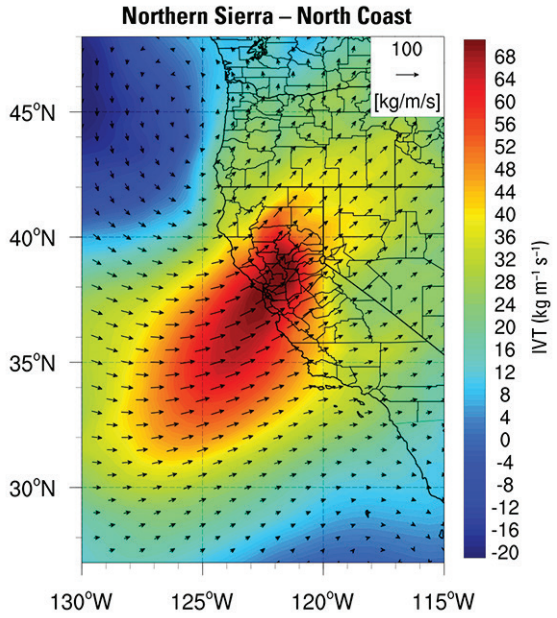

Figure 10 The difference between IVT composites for ARs associated with extreme rainfall events in northern Sierra and the north coast (panel **D** subtracted from panel **E** in Figure 9). The largest differences between ARs that yield extreme rainfall along the coast of northern California and those that yield extreme rainfall over northern Sierra are located at the SFBA gap.

documented in the literature, because at many locations just one storm contributes up to 25% of the total annual rainfall. Our study also highlights differences between extreme rainfall characteristics in different regions of California and identifies some characteristics of ARs that contribute the most to extreme rainfall events.

Northern California generally receives a larger number of rainfall events annually with longer durations but smaller event-maximum rainfall intensities than does southern California. Almost all across California, event durations dominate rainfall-event precipitation totals more strongly than maximum intensities. Nonetheless, in coastal regions, maximum intensities also play important roles in determining event-total rainfall. Across California, ARs contribute to extreme rainfall, with larger contributions in northern than southern California. In northern California, AR-related extreme-rainfall events are slightly shorter than non-AR extreme events on average, but have larger maximum intensities, enough larger so that AR extremes have larger event totals than do non-AR extremes. In contrast, in the Transverse Ranges of southern California, AR-related extreme rainfall events are both longer and have higher maximum intensities than non-AR extreme events, which together yield the largest extreme event-total rainfalls in the state.

ARs associated with extreme rainfall events in northern California have stronger IVTs than those in southern California, following the general pattern of AR landfalls with stronger IVTs in northern than in southern California (Rutz et al. 2014: 201; Dettinger et al. 2018). Vapor transports in ARs that yield extreme rainfall along the northern California coast, on average, approach somewhat more from the southwest than other directions, and thus are perpendicular to coastal topography in the northern Coastal Ranges. The vapor transports in southern California ARs associated with extreme rainfall, on the other hand, approach more from the south, and thus also perpendicular to the Transverse Ranges in southern California. These orientations particularly favor the generation of orographic precipitation in these regions.

The SFBA gap in coastal northern California topography plays an important role in northern California's inland precipitation distributions by allowing more IVT from AR landfalls near San Francisco to penetrate into the Central Valley and Sierra Nevada. ARs that instead cross the major coast ranges lose more of their vapor through rain-out before reaching the Sierra Nevada. Here, we extend on these results found by previous studies (Neiman et al. 2013; White et al. 2015) and show that the largest differences in IVT magnitudes of ARs that yield extreme rainfall along the north coast and northern Sierra Nevada are located at this gap, highlighting the importance of the gap and ARs penetrating there for flood risks and water-reliability in the northern Sierra Nevada, Central Valley, and, ultimately, in the Bay and Delta.

These kinds of findings provide improved scientific foundations that potentially can be valuable for water-management and flood-risk-mitigation strategies throughout the state. They also offer insights into storms that pose the greatest flood and landslide risks, as well as the storms that are most likely to prevent or mitigate drought conditions.

One of the major limitations of our current study is its lack of attention to frozen precipitation. Deployment of more instruments that can reliably measure both frozen and unfrozen precipitation at hourly levels in regions with frozen precipitation will be a valuable addition to the existing observation network. Higher-resolution models and targeted observation networks (White et al. 2013; Ralph et al. 2014, 2016) will be needed to more fully characterize both the effects and the ability to forecast the effects of topography and finer-scale atmospheric mechanisms on extreme AR-related rainfall events.

ACKNOWLEDGMENTS

The AR chronology data set used in this study was retrieved from *http://www.inscc.utah.edu/~rutz/ar_catalogs/merra_0.5/*. Hourly precipitation observations from the RAWS and CIMIS networks were accessed from *https://raws.dri.edu/* and *http://www.cimis.water.ca.gov/*, respectively. A list of precipitation observation stations and their locations is presented in Table A1. This study is supported by the US Army Corps of Engineers (USACE)-Cooperative Ecosystem Studies Unit (CESU) as part of the Forecast Informed Reservoir Operations (FIRO) under grant W912HZ-15-2-0019. MD's participation was supported by the USGS National Research Program with funding from the Sonoma County Water Agency. NSO's participation was supported by the National Oceanic and Atmospheric

Administration's Climate Program Office through Grant NA11OAR4310150 with the California Nevada Applications Program.

REFERENCES

Albano CM, Dettinger MD, Soulard CE. 2017. Influence of atmospheric rivers on vegetation productivity and fire patterns in the southwestern U.S. J Geophys Res Biogeosciences 122(2):2016JG003608. *https://doi.org/10.1002/2016JG003608*

Brown TJ, Horel JD, McCurdy GD, Fearon MG. 2011. What is the appropriate RAWS network? Report No.: CEFA Report 11-01. [Reno (NV)]: National Wildfire Coordinating Group [cited 2018 May 15]. Available from: *https://www.nwcg.gov/sites/default/files/publications/pms1003.pdf*

Dettinger M. 2011. Climate change, atmospheric rivers, and floods in California—a multimodel analysis of storm frequency and magnitude changes. J Am Water Resour Assoc 47(3):10. *https://doi.org/10.1111/j.1752-1688.2011.00546.x*

Dettinger M. 2016. Historical and future relations between large storms and droughts in California. San Franc Estuary Watershed Sci 14(2). [cited 2018 March 20]. *https://doi.org/10.15447/sfews.2016v14iss2art1*

Dettinger MD. 2013. Atmospheric rivers as drought busters on the U.S. West Coast. J Hydrometeorol 14(6):1721–1732. *https://doi.org/10.1175/JHM-D-13-02.1*

Dettinger MD, Ingram BL. 2013. The coming megafloods. Sci Am 308(1):64–71. *https://doi.org/10.1038/scientificamerican0113-64*

Dettinger MD, Ralph FM, Das T, Neiman PJ, Cayan DR. 2011. Atmospheric rivers, floods and the water resources of California. Water 3(2):445–478. *https://doi.org/10.3390/w3020445*

Dettinger MD, Ralph FM, Rutz JJ. 2018. Empirical return periods of the most intense vapor transports during historical atmospheric river landfalls on the U.S. West Coast. J Hydrometeorol 19(8):1363–1377. *https://doi.org/10.1175/JHM-D-17-0247.1*

Espinoza V, Waliser DE, Guan B, Lavers DA, Ralph FM. 2018. Global analysis of climate change projection effects on atmospheric rivers. Geophys Res Lett. 45(9):4299–4308. *https://doi.org/10.1029/2017GL076968*

FIRO Steering Committee. 2017. Preliminary viability assessment of Lake Mendocino forecast informed reservoir operations. [cited 2018 04 20]. Available from: *http://cw3e.ucsd.edu/firo-preliminary-viability-assessment-for-lake-mendocino/*

Glossary of Meteorology. 2017. Atmospheric river. [cited 2018 May 20]. Available from: *http://glossary.ametsoc.org/wiki/Atmospheric_river*

Guan B, Molotch NP, Waliser DE, Fetzer EJ, Neiman PJ. 2010. Extreme snowfall events linked to atmospheric rivers and surface air temperature via satellite measurements. Geophys Res Lett 37(20):L20401. *https://doi.org/10.1029/2010GL044696*

https://doi.org/10.15447/sfews.2018v16iss4art1

Hagos SM, Leung LR, Yoon J-H, Lu J, Gao Y. 2016. A projection of changes in landfalling atmospheric river frequency and extreme precipitation over western North America from the Large Ensemble CESM simulations. Geophys Res Lett 43(3):2015GL067392. *https://doi.org/10.1002/2015GL067392*

Hughes M, Mahoney KM, Neiman PJ, Moore BJ, Alexander M, Ralph FM. 2014. The landfall and inland penetration of a flood-producing atmospheric river in Arizona. Part II: sensitivity of modeled precipitation to terrain height and atmospheric river orientation. J Hydrometeorol 15(5):1954–1974. *https://doi.org/10.1175/JHM-D-13-0176.1*

Kim J, Waliser DE, Neiman PJ, Guan B, Ryoo J-M, Wick GA. 2013. Effects of atmospheric river landfalls on the cold season precipitation in California. Clim Dyn 40(1–2):465–474. *https://doi.org/10.1007/s00382-012-1322-3*

Konrad CP, Dettinger MD. 2017. Flood runoff in relation to water vapor transport by atmospheric rivers over the western United States, 1949–2015. Geophys Res Lett 44(22):2017GL075399. *https://doi.org/10.1002/2017GL075399*

Lamjiri MA, Dettinger MD, Ralph FM, Guan B. 2017. Hourly storm characteristics along the U.S. West Coast: role of atmospheric rivers in extreme precipitation. Geophys Res Lett 44(13):2017GL074193. *https://doi.org/10.1002/2017GL074193*

Lavers DA, Allan RP, Villarini G, Lloyd-Hughes B, Brayshaw DJ, Wade AJ. 2013. Future changes in atmospheric rivers and their implications for winter flooding in Britain. Environ Res Lett 8(2013):031006. *https://doi.org/10.1088/1748-9326/8/3/031006*

Lavers DA, Villarini G. 2015. The contribution of atmospheric rivers to precipitation in Europe and the United States. J Hydrol 522:382–390. *https://doi.org/10.1016/j.jhydrol.2014.12.010*

Lavers DA, Waliser DE, Ralph FM, Dettinger MD. 2016. Predictability of horizontal water vapor transport relative to precipitation: Enhancing situational awareness for forecasting western U.S. extreme precipitation and flooding. Geophys Res Lett 43(5):2016GL067765. *https://doi.org/10.1002/2016GL067765*

Mann HB, Whitney DR. 1947. On a test of whether one of two random variables is stochastically larger than the other. Ann Math Stat 18(1):50–60. *https://doi.org/10.1214/aoms/1177730491*

Myrick DT, Horel JD. 2008. Sensitivity of surface analyses over the western United States to RAWS observations. Weather Forecast 23(1):145–158. *https://doi.org/10.1175/2007WAF2006074.1*

Neiman PJ, Hughes M, Moore BJ, Ralph FM, Sukovich EM. 2013. Sierra barrier jets, atmospheric rivers, and precipitation characteristics in northern California: a composite perspective based on a network of wind profilers. Mon Weather Rev 141(12):4211–4233. *https://doi.org/10.1175/MWR-D-13-00112.1*

Neiman PJ, Ralph FM, Wick GA, Lundquist JD, Dettinger MD. 2008. Meteorological characteristics and overland precipitation impacts of atmospheric rivers affecting the West Coast of North America based on eight years of SSM/I satellite observations. J Hydrometeorol 9(1):22–47. *https://doi.org/10.1175/2007JHM855.1*

Neiman PJ, Schick LJ, Ralph FM, Hughes M, Wick GA. 2011. Flooding in western Washington: the connection to atmospheric rivers. J Hydrometeorol 12(6):1337–1358. *https://doi.org/10.1175/2011JHM1358.1*

Oakley NS, Lancaster JT, Hatchett BJ, Stock J, Ralph FM, Roj S, Lukashov S. 2018. A 22-year climatology of cool season hourly precipitation conducive to shallow landslides in California. Earth Interact 22(14):1–35. *https://doi.org/10.1175/EI-D-17-0029.1*

Oakley NS, Lancaster JT, Kaplan ML, Ralph FM. 2017. Synoptic conditions associated with cool season post-fire debris flows in the Transverse Ranges of southern California. Nat Hazards 88(1):327–354. *https://doi.org/10.1007/s11069-017-2867-6*

Paltan H, Waliser D, Lim WH, Guan B, Yamazaki D, Pant R, Dadson S. 2017. Global floods and water availability driven by atmospheric rivers. Geophys Res Lett 44(20):10,387–10,395. *https://doi.org/10.1002/2017GL074882*

Polade SD, Gershunov A, Cayan DR, Dettinger MD, Pierce DW. 2017. Precipitation in a warming world: Assessing projected hydro-climate changes in California and other Mediterranean climate regions. Sci Rep 7(1):10783. *https://doi.org/10.1038/s41598-017-11285-y*

Ralph FM, Coleman T, Neiman PJ, Zamora RJ, Dettinger MD. 2013. Observed impacts of duration and seasonality of atmospheric-river landfalls on soil moisture and runoff in coastal northern California. J Hydrometeorol 14(2):443–459. *https://doi.org/10.1175/JHM-D-12-076.1*

Ralph FM, Dettinger MD, Cairns MM, Galarneau TJ, Eylander J. 2018. Defining "atmospheric river": How the Glossary of Meteorology helped resolve a debate. Bull Am Meteorol Soc 99(4):837–839. *https://doi.org/10.1175/BAMS-D-17-0157.1*

Ralph FM, Dettinger MD, White AB, Reynolds DW, Cayan D, Schneider TL, Cifelli R, Redmond K, Anderson ML, Gherke F, et al. 2014. A vision for future observations for western U.S. extreme precipitation and flooding. J Contemp Water Res Educ (153):16–32. *https://doi.org/10.1111/j.1936-704X.2014.03176.x*

Ralph FM, Neiman PJ, Kingsmill DE, Persson POG, White AB, Strem ET, Andrews ED, Antweiler RC. 2003. The impact of a prominent rain shadow on flooding in California's Santa Cruz mountains: a CALJET case study and sensitivity to the ENSO cycle. J Hydrometeorol 4(6):1243–1264. *https://doi.org/10.1175/1525-7541(2003)004<1243:TIOAPR>2.0.CO;2*

Ralph FM, Neiman PJ, Wick GA. 2004. Satellite and CALJET aircraft observations of atmospheric rivers over the eastern North Pacific Ocean during the winter of 1997/98. Mon Weather Rev 132(7):1721–1745. *https://doi.org/10.1175/1520-0493(2004)132<1721:SACAOO>2.0.CO;2*

Ralph FM, Neiman PJ, Wick GA, Gutman SI, Dettinger MD, Cayan DR, White AB. 2006. Flooding on California's Russian River: role of atmospheric rivers. Geophys Res Lett 33(13):L13801. *https://doi.org/10.1029/2006GL026689*

Ralph FM, Prather KA, Cayan D, Spackman JR, DeMott P, Dettinger M, Fairall C, Leung R, Rosenfeld D, Rutledge S, et al. 2016. CalWater field studies designed to quantify the roles of atmospheric rivers and aerosols in modulating U.S. West Coast precipitation in a changing climate. Bull Am Meteorol Soc 97(7):1209–1228. *https://doi.org/10.1175/BAMS-D-14-00043.1*

Ralph FM, Wilson AM, Shulgina T, Kawzenuk B, Sellars S, Rutz JJ, Lamjiri MA, Barnes EA, Gershunov A, Guan B, et al. 2018b. ARTMIP-early start comparison of atmospheric river detection tools: how many atmospheric rivers hit northern California's Russian River watershed? Clim Dyn *https://doi.org/10.1007/s00382-018-4427-5*

Rutz JJ, Steenburgh WJ, Ralph FM. 2014. Climatological characteristics of atmospheric rivers and their inland penetration over the western United States. Mon Weather Rev 142(2):905–921. *https://doi.org/10.1175/MWR-D-13-00168.1*

Shields CA, Rutz JJ, Leung L-Y, Ralph FM, Wehner M, Kawzenuk B, Lora JM, McClenny E, Osborne T, Payne AE, et al. 2018. Atmospheric river tracking method intercomparison project (ARTMIP): project goals and experimental design. Geosci Model Dev 11(6):2455–2474. *https://doi.org/10.5194/gmd-11-2455-2018*

Waliser D, Guan B. 2017. Extreme winds and precipitation during landfall of atmospheric rivers. Nat Geosci 10(3):179–183. *https://doi.org/10.1038/ngeo2894*

Warner MD, Mass CF, Salathé EP. 2014. Changes in winter atmospheric rivers along the North American West Coast in CMIP5 climate models. J Hydrometeorol 16(1):118–128. *https://doi.org/10.1175/JHM-D-14-0080.1*

White AB, Anderson ML, Dettinger MD, Ralph FM, Hinojosa A, Cayan DR, Hartman RK, Reynolds DW, Johnson LE, Schneider TL, et al. 2013. A twenty-first-century California observing network for monitoring extreme weather events. J Atmospheric Ocean Technol 30(8):1585–1603. *https://doi.org/10.1175/JTECH-D-12-00217.1*

White AB, Neiman PJ, Creamean JM, Coleman T, Ralph FM, Prather KA. 2015. The impacts of California's San Francisco Bay Area gap on precipitation observed in the Sierra Nevada during HMT and CalWater. J Hydrometeorol 16(3):1048–1069. *https://doi.org/10.1175/JHM-D-14-0160.1*

Young AM, Skelly KT, Cordeira JM. 2017. High-impact hydrologic events and atmospheric rivers in California: an investigation using the NCEI storm events database. Geophys Res Lett 44(7):2017GL073077. *https://doi.org/10.1002/2017GL073077*

Zhu Y, Newell RE. 1998. A proposed algorithm for moisture fluxes from atmospheric rivers. Mon Weather Rev 126(3):725–735. *https://doi.org/10.1175/1520-0493(1998)126<0725:APAFMF>2.0.CO;2*

https://doi.org/10.15447/sfews.2018v16iss4art1